Responses of Freshwater Calcifiers to Carbon-Dioxide-Induced Acidification

Aaron T. Ninokawa [1,2,*] and **Justin Ries** [3,4]

1   Bodega Marine Laboratory, University of California, Davis, Bodega Bay, CA 94923, USA
2   Friday Harbor Laboratories, University of Washington, Friday Harbor, WA 98250, USA
3   Department of Marine and Environmental Sciences, Northeastern University, Boston, NA 02115, USA
4   Tahoe Environmental Research Center, University of California, Davis, Incline Village, NV 89451, USA
*   Correspondence: anino@uw.edu

Abstract: Increased anthropogenic carbon dioxide (CO_2) in the atmosphere can enter surface waters and depress pH. In marine systems, this phenomenon, termed ocean acidification (OA), can modify a variety of physiological, ecological, and chemical processes. Shell-forming organisms are particularly sensitive to this chemical shift, though responses vary amongst taxa. Although analogous chemical changes occur in freshwater systems via absorption of CO_2 into lakes, rivers, and streams, effects on freshwater calcifiers have received far less attention, despite the ecological importance of these organisms to freshwater systems. We exposed four common and widespread species of freshwater calcifiers to a range of pCO_2 conditions to determine how CO_2-induced reductions in freshwater pH impact calcium carbonate shell formation. We incubated the signal crayfish, *Pacifastacus leniusculus*, the Asian clam, *Corbicula fluminea*, the montane pea clam, *Pisidium* sp., and the eastern pearlshell mussel, *Margaritifera margaritifera*, under low pCO_2 conditions (pCO_2 = 616 ± 151 μatm; pH = 7.91 ± 0.11), under moderately elevated pCO_2 conditions (pCO_2 = 1026 ± 239 uatm; pH = 7.67 ± 0.10), and under extremely elevated pCO_2 conditions (pCO_2 = 2380 ± 693 uatm; pH = 7.32 ± 0.12). Three of these species exhibited a negative linear response to increasing pCO_2 (decreasing pH), while the fourth, the pea clam, exhibited a parabolic response. Additional experiments revealed that feeding rates of the crayfish decreased under the highest pCO_2 treatment, potentially contributing to or driving the negative calcification response of the crayfish to elevated pCO_2 by depriving them of energy needed for biocalcification. These results highlight the potential for freshwater taxa to be deleteriously impacted by increased atmospheric pCO_2, the variable nature of these responses, and the need for further study of this process in freshwater systems.

Keywords: ocean acidification; freshwater acidification; freshwater calcifier; carbon dioxide; calcification; biomineralization; Lake Tahoe

1. Introduction

Increased partial pressure of atmospheric carbon dioxide (pCO_2) drives large scale alterations to environmental systems. In particular, this additional CO_2 can enter surface waters and perturb the aquatic carbonate system, lowering pH, carbonate ion concentration ($[CO_3^{2-}]$), and the saturation state of water with respect to calcium carbonate ($CaCO_3$). In marine systems, this process, termed ocean acidification, can impair tissue and shell growth and alter the behavior of many marine species, yielding ecological changes across a range of spatial, temporal, and trophic scales [1].

Calcifying organisms, those producing calcium carbonate shells or skeletons, are especially sensitive to CO_2-induced changes in carbonate system chemistry, although the drivers of this sensitivity can be complex [2–4]. In many taxa, calcium carbonate material is produced more slowly under increased pCO_2 [1,5], with shell and skeletal material produced under these conditions tending to be weaker [6,7]. Some species, however, grow faster under increased pCO_2 or can maintain or enhance the quality of their shell or skeletal

material [5,8]. In many cases, the effects of pCO_2 operate indirectly, often via pathways related to pH, bicarbonate, or carbonate ions [3,9]. Indeed, the diversity of responses to increased pCO_2 complicates the process of generalizing how calcifying taxa will respond to CO_2-induced acidification in the future [4].

Although there have been many studies examining effects of CO_2-induced acidification on marine species, far fewer have considered responses of freshwater species. Freshwater typically has lower alkalinity, or chemical buffering capacity, which makes the $CaCO_3$ saturation state of freshwater less than that of seawater for equivalent pCO_2 conditions, while also rendering the carbonate chemistry of freshwater systems more sensitive to variations in atmospheric pCO_2 than that of marine systems [10,11]. Freshwater species, for example, will experience larger shifts in pH and lower absolute $CaCO_3$ saturation states than their marine analogs for a given increase in anthropogenic CO_2. The lower alkalinity of freshwater systems also makes the carbonate chemistry of these systems more vulnerable to diurnal and seasonal cycles in photosynthesis and respiration than marine systems [10]. It is, therefore, possible that freshwater calcifiers will be more sensitive than marine calcifiers to equivalent shifts in atmospheric pCO_2. Alternatively, the naturally higher variability in carbonate chemistry and lower absolute saturation state of freshwater systems could select for freshwater calcifying taxa that are relatively resilient to CO_2-induced perturbations to carbonate system chemistry.

Although past research has examined responses of freshwater calcifying species to elevated aqueous CO_2, most of this earlier work was conducted with the aim of understanding physiological acid–base dynamics within the organisms themselves, rather than understanding the impacts of CO_2-induced acidification on shell and skeletal formation. Thus, much of this prior work employed unrealistically high pCO_2 conditions that exceed projected end-of-century CO_2 partial pressures by tens of thousands of microatmospheres (μatm), resulting in unrealistic pH reductions in the order of 2 units [12]. Furthermore, among the modest number of studies where pCO_2 treatments reflected realistic future scenarios, prior work has focused on shifts in primary productivity by phytoplankton and changes in food quality [10] as driving calcifier performance, rather than on the direct effects of CO_2-induced changes in freshwater carbonate chemistry. Therefore, to determine the effect of increased atmospheric pCO_2 on calcifying invertebrates in the context of increasing anthropogenic pCO_2, we reared four species of freshwater calcifiers under three atmospheric pCO_2 conditions that bracket the range of conditions expected to occur over the next two centuries given the range of future emissions scenarios [13].

2. Materials and Methods

This project was conducted at the University of California, Davis, Tahoe Environmental Research Center (Tahoe City Field Station) and Lot #4 of Alpine Meadows, CA, USA between December 2020 and August 2021. The freshwater employed in the flow-through CO_2-induced acidification experiments was sourced from Burton Spring, a tributary of Lake Tahoe. The carbonate chemistry of the treatments was controlled by maintaining constant pH in three 800 L sumps with a pH-stat system (American Marine Inc. Pinpoint pH Controller) that reduced pH by dosing pure compressed CO_2 with a solenoid-valve controlled gas regulator (FZone Pro Series CO_2 Regulator), or increased pH by dosing ambient air through an air pump (Simply Deluxe Electromagnetic Air Pump). The compressed CO_2 and compressed air were sparged into the sumps and treatments tanks with flexible, microporous bubbling tubes that were designed to expedite equilibration between aqueous and gas phases. Spring water (filtered to 10 μm) entered the sumps at a rate of 1 L min^{-1} to minimize accumulation of metabolic byproducts and prevent depletion of alkalinity and calcium ions through the calcification process. The sumps and experimental tanks were covered with plastic sheeting and plastic lids, respectively, to prevent room air from equilibrating with the water in the sumps and the experimental treatments. The water within each of the three sump systems was recirculated through 12–40 L tanks (3 sumps × 12 tanks = 36 tanks total), with the recirculating water passing through an

activated carbon filter (changed biweekly) before entering the tanks and through 10 L of loose activated carbon media (changed monthly) before re-entering the sump (Figure 1). Temperature varied naturally with the seasons but was maintained below 22 °C with chillers and the addition of frozen spring water.
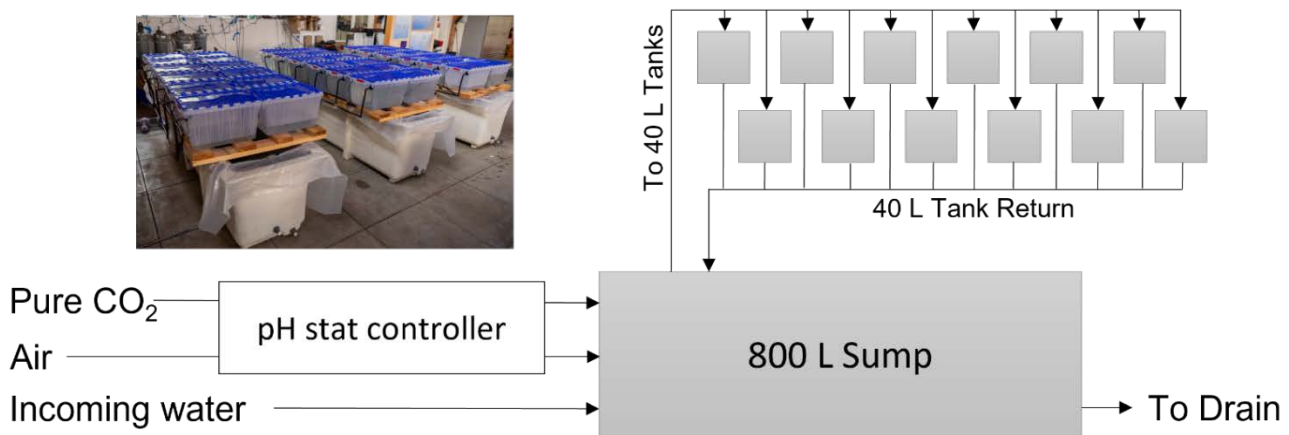
Figure 1. Schematic diagram of one of the three identical pCO_2 control systems used in the experiment. Fresh spring water flowed continuously through the main sump and recirculated amongst the experimental tanks. A pH stat controller added either pure CO_2 or ambient air as required to maintain water pH within the target range. The image in the top left shows arrangement of all three pCO_2 treatment systems in the laboratory.

Water chemistry was measured three times per week with a Thermo Scientific Orion Star A329 Multiparameter Meter. Oxygen (Orion RDO Optical Dissolved Oxygen Probe) and pH sensors (Atlas Scientific Spear-tip pH) were calibrated daily in air-equilibrated water and with NIST-traceable NBS buffers (pH 7 and 10), respectively. The conductivity probe (Duraprobe) was calibrated every other week with Oakton 84 and 1413 µS cm^{-1} standards. Discrete 200 mL water samples were collected from the three sumps during each of these sampling events and frozen until they could be analyzed for alkalinity with a Metrohm 855 Robotic Titrosampler.

In addition to these higher frequency measurements, discrete 500 mL water samples were collected weekly from each of the 36 tanks and analyzed at the Tahoe Environmental Research Center (Incline Village Field Station) for dissolved inorganic carbon (DIC) on a Lachat IL 500 TOC instrument. The 'seacarb' package in *R* was used to calculate total alkalinity (TA) from these lower frequency DIC and pH measurements using constants from Waters et al. [14]. This information was used to define the linear relationship between specific conductance and TA for water employed in this experiment (Figure 2). We then used this relationship to estimate TA from the higher frequency measurement of water-specific conductance (described above). The calculated TA was 96 ± 0.3% (mean ± se, n = 149) of the measured alkalinity described above. Given this good agreement between calculated and measured alkalinity, we then used these higher frequency measurements of pH and conductivity-estimated alkalinity, along with measured temperature and total dissolved solids, to calculate carbonate system parameters for each tank throughout the duration of the experiment. The saturation state of calcite ($\Omega_{calcite}$) was calculated assuming that the calcium concentration was half the alkalinity as calcium concentrations in the Lake Tahoe area tend to be between 0.5 and 1 times the alkalinity [15]. Small deviations in Ca^{2+} concentration from this relationship will not materially impact the calculated saturation states or the interpretation of the results.
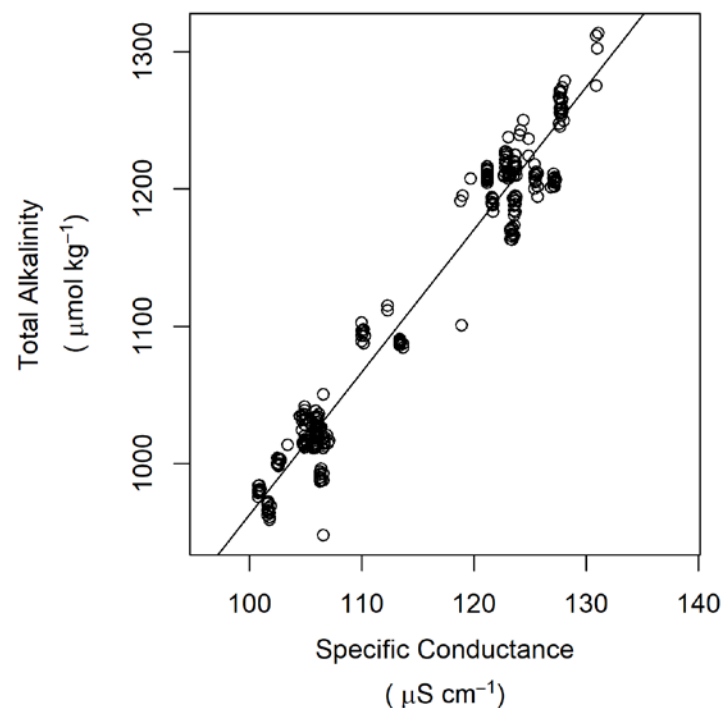
Figure 2. Relationship between specific conductance and total alkalinity for water samples obtained from this experiment. The linearity of this relationship allowed the calculation of total alkalinity (for carbonate system calculations) from higher frequency measurements of specific conductance.

The species investigated in this experiment were collected from the field and acclimated to laboratory conditions for at least 5 days prior to starting the experiments. Signal crayfish, *Pacifastacus leniusculus*, were collected from Pomin Park in Tahoe City, CA, USA, in late April 2021. Two cohorts of Asian clams, *Corbicula fluminea*, were collected from Marla Bay and Lakeside near Stateline, NV, on 15 April 2021 and 24 May 2021.

Two cohorts of pea clams, *Pisidium* sp., were collected from a spring feeding into the Truckee River near Polaris, CA, on 13 May 2021 and 19 June 2021. Pearlshell mussels, *Margaritifera margaritifera*, were collected from a lake near Jupiter, Florida, in early May 2021. Bivalves were held in three of the 40 L tanks per CO_2 treatment while crayfish were held in a different set of three tanks (9 tanks total per species). Remaining tanks (6 per pCO_2 treatment) were used for respiration and feeding trials described below. Bivalves were fed a commercially available Shellfish Diet twice daily at a concentration of 5 mL per 40 L of tank water. Crayfish were fed 1×1 cm dehydrated algae sheets and raw shrimp ad libitum every other day, with uneaten food removed at the time of feeding. All tanks were cleaned of accumulated solid waste three or four times per week.

Organisms remained within the tanks for the duration of the experiment and net calcification rates were calculated as the fractional change in shell mass determined from buoyant weights at the beginning and end of the experiment, normalized to a 30-day interval. Shell mass was calculated from buoyant weight measurements, where the density of the water was determined daily by the air and buoyant weights of glass bead standards (measured daily) with densities of either 2.55 or 2.23 g cm^{-3} [16]. Daily buoyant and dry weights of four half shells of *Corbicula fluminea* and two half shells of *Margaritifera margaritifera* revealed that these species had shell densities of 2.81 and 2.71 g cm^{-3}, respectively and these values were used for calculating shell mass from buoyant weight [16]. A shell density of 2.71 g cm^{-3} was used for calculating the crayfish shell mass from their buoyant weight. Because crayfish transport calcium carbonate between their external shell and internal gastrolith during the molting process [17], crayfish that, at the conclusion of the incubation, had recently molted and had not yet remineralized their shell (i.e., the shell was soft) were excluded from further analysis. Due to their small size, net calcification rate of pea clams

was calculated as the fractional change in wet mass between the beginning and end of the experiment normalized to a 30-day interval, measured with a Sartorius 2120T microbalance after removing excess water from the shell with lint-free wipes and allowing the clams to air dry for precisely 15 min prior to weighing. Net calcification rates were analyzed with a maximum likelihood routine fitting various functional models identified previously [5], including linear, parabolic, and threshold (exponential) relationships with average pCO_2 during the incubation period using individuals as replicates. The statistically significant model with the lowest AIC was selected as the best one to describe the relationship between pCO_2 and net calcification rate.

At the conclusion of the growth experiments, additional experiments were conducted to test whether CO_2-induced changes in carbonate chemistry impaired crayfish feeding. A new batch of live crayfish prey (pea clams) was collected and acclimated to the pCO_2 treatments for three days. Five pea clams of comparable size were placed in each of six tanks per pCO_2 treatment with a single crayfish per tank. The number of pea clams consumed after each 25 min trial was recorded. The respiration rates of the crayfish were also obtained to determine whether pCO_2-induced changes in water chemistry altered metabolic rates and, therefore, feeding requirements. Before the feeding trials, we placed each crayfish in a sealed incubation vessel and measured the change in oxygen concentration during the incubation time with the Orion RDO dissolved oxygen probe. Respiration and feeding trials both took place at night in the dark, as this is when the crayfish are most active.

3. Results

The freshwater calcifying organisms in this study were exposed to pCO_2 conditions approximately double and quadruple those of average present-day conditions. Mean daily $pCO_2 \pm$ SD (calculated from pH, total alkalinity, TDS, and temperature) across all tanks in the control, intermediate, and high treatments were 616 ± 151 µatm, 1026 ± 239, and 2380 ± 693 (Figure 3d, Table 1, n = 35 sampling days), respectively, corresponding to mean daily pH $\pm$ SD of 7.91 ± 0.11, 7.67 ± 0.10, and 7.32 ± 0.12 (Figure 3b, Table 1, n = 35 sampling days). Daily mean alkalinity decreased throughout the course of the experiment from 1272 to 927 µmol kg^{-1} (Figure 3c), probably due to increased contribution of snowmelt relative to groundwater through the spring–summer transition. This trend was accompanied by an increase in daily mean temperature from 12.2 to 21.4 °C (Figure 3a). The relationship between specific conductance (SC, µS cm^{-1}) and total alkalinity (TA, µmol kg^{-1}) was TA $= -75.46 + 10.38 * $ SC ($R^2 = 0.96$, $F_{1314} = 6937$, $p < 0.001$).

Table 1. Average treatment conditions during the experiment. Measurements are the mean (standard deviation) of 12 tanks per treatment over 35 sampling days.

Parameter	Units	Low pCO_2	Intermediate pCO_2	High pCO_2
Temperature	°C	17.9 (2.6)	17.9 (2.5)	17.6 (2.5)
Specific conductance	µS cm^{-1}	113 (11)	111 (10)	113 (11)
Dissolved oxygen	µmol L^{-1}	232 (13)	230 (13)	227 (9)
pH (NBS scale)		7.91 (0.11)	7.67 (0.10)	7.32 (0.12)
Total alkalinity	µmol kg^{-1}	1098 (116)	1078 (102)	1093 (110)
pCO_2	µatm	616 (151)	1026 (239)	2380 (693)
[HCO$_3^-$]	µmol kg^{-1}	1088 (114)	1072 (102)	1090 (110)
[CO$_3^{2-}$]	µmol kg^{-1}	4.7 (1.4)	2.7 (0.7)	1.2 (0.4)
$\Omega_{aragonite}$		0.50 (0.16)	0.28 (0.08)	0.13 (0.04)
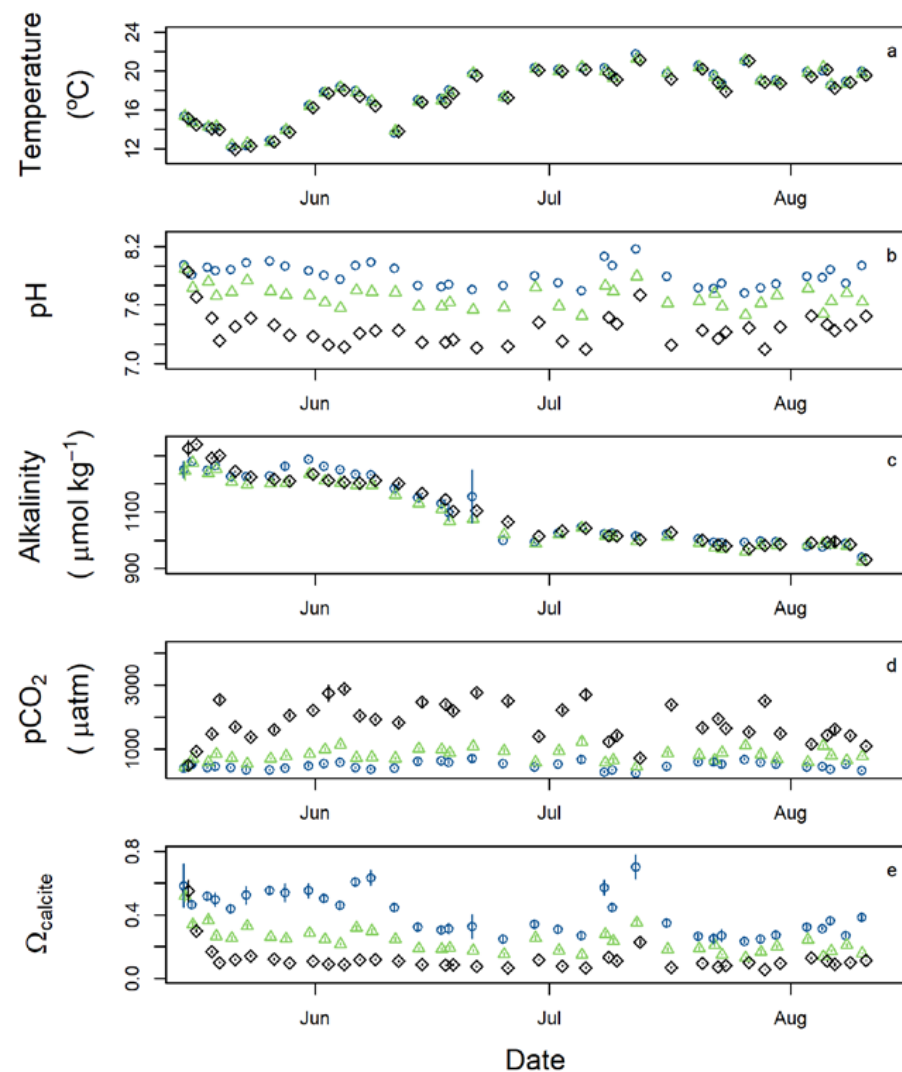
Figure 3. Average daily conditions within the experimental replicate tanks throughout the duration of the experiment. Blue circles indicate the low pCO_2 treatment, green triangles indicate the intermediate pCO_2 treatment, and black diamonds indicate the high pCO_2 treatment. Vertical bars show the standard deviation of all 12 tanks at each pCO_2 treatment.

Net calcification rates of the four species as a function of pCO_2 followed two general response types (Tables 2 and 3). Net calcification rates of *Pacifastacus leniusculus* (Figure 4a), *Corbicula fluminea* (Figure 4b), and *Margaritifera margaritifera* (Figure 4c) exhibited a linear decline in net calcification with increasing pCO_2 (decreasing pH). Net calcification rate of *Pisidium* sp. exhibited a parabolic relationship with pCO_2, in which maximum rates of net calcification were observed in the intermediate pCO_2 treatment (Figure 4d).

Table 2. Net calcification rates (fractional change in buoyant or wet weight normalized to a 30-day growth interval) in each treatment for each species during the experiment. Values reported are mean (standard error), sample size.

Species	Low pCO_2	Intermediate pCO_2	High pCO_2
P. leniusculus	−0.007 (0.003), 10	−0.009 (0.002), 15	−0.019 (0.003), 8
C. fluminea	−0.018 (0.004), 33	−0.019 (0.004), 31	−0.032 (0.004), 31
M. margaritifera	−0.087 (0.006), 25	−0.082 (0.008), 19	−0.108 (0.008), 18
Pisidium sp.	0.003 (0.003), 29	0.013 (0.003), 35	0.007 (0.003), 21

Table 3. Parameter estimates for tested models describing the relationship between net calcification rate and pCO_2. Linear models took the form net calcification rate = b0 + b1 ∗ pCO_2. Parabolic models took the form net calcification rate = b0 + b1 ∗ pCO_2 + b2 ∗ $(pCO_2)^2$. Exponential models took the form net calcification rate = b0 + b1 ∗ e^{b2*pCO_2}. Bold rows indicate statistically significant model (α = 0.05) with the lowest AIC value for a given species.

Species	Model	b0	b1	b2	R2	RMSE	F-Statistic	*p*-Value	AIC
P. leniusculus	**linear**	-1.79×10^{-3}	-5.42×10^{-6}		**0.257**	**0.008**	**10.71 (1, 31)**	**0.0026**	**−217.18**
P. leniusculus	exponential	-1.10×10^{-4}	-4.71×10^{-3}	4.41×10^{-4}	0.260	0.008	5.29 (2, 30)	0.0104	−215.33
P. leniusculus	parabolic	-5.84×10^{-3}	-4.32×10^{-7}	-1.19×10^{-9}	0.260	0.008	5.27 (2, 30)	0.0105	−215.32
C. fluminea	**linear**	-1.35×10^{-2}	-5.76×10^{-6}		**0.052**	**0.024**	**5.13 (1, 93)**	**0.0258**	**−433.29**
C. fluminea	exponential	1.32×10^{-2}	-2.80×10^{-2}	1.49×10^{-4}	0.050	0.024	2.4 (2, 92)	0.0963	−431.04
C. fluminea	parabolic	2.53×10^{-3}	-2.80×10^{-5}	5.64×10^{-9}	0.067	0.024	3.3 (2, 92)	0.0410	−432.78
M. margaritifera	**linear**	-7.38×10^{-2}	-1.15×10^{-5}		**0.099**	**0.032**	**6.6 (1, 60)**	**0.0126**	**−243.26**
M. margaritifera	exponential	-4.67×10^{-2}	-3.66×10^{-2}	8.29×10^{-5}	0.044	0.033	0.52 (2, 59)	0.5973	−229.62
M. margaritifera	parabolic	-7.86×10^{-2}	-4.40×10^{-6}	-1.90×10^{-9}	0.100	0.032	3.27 (2, 59)	0.0447	−241.29
Pisidium sp.	linear	8.06×10^{-3}	-5.23×10^{-8}		0.000	0.017	0.001 (1, 83)	0.9815	−442.70
Pisidium sp.	exponential	-7.37×10^{-3}	1.54×10^{-2}	-3.09×10^{-6}	0.000	0.017	0.0002 (2, 82)	0.9998	−440.70
***Pisidium* sp.**	**parabolic**	-1.68×10^{-2}	3.37×10^{-5}	-8.68×10^{-9}	**0.076**	**0.017**	**3.393 (2, 82)**	**0.0383**	**−447.46**
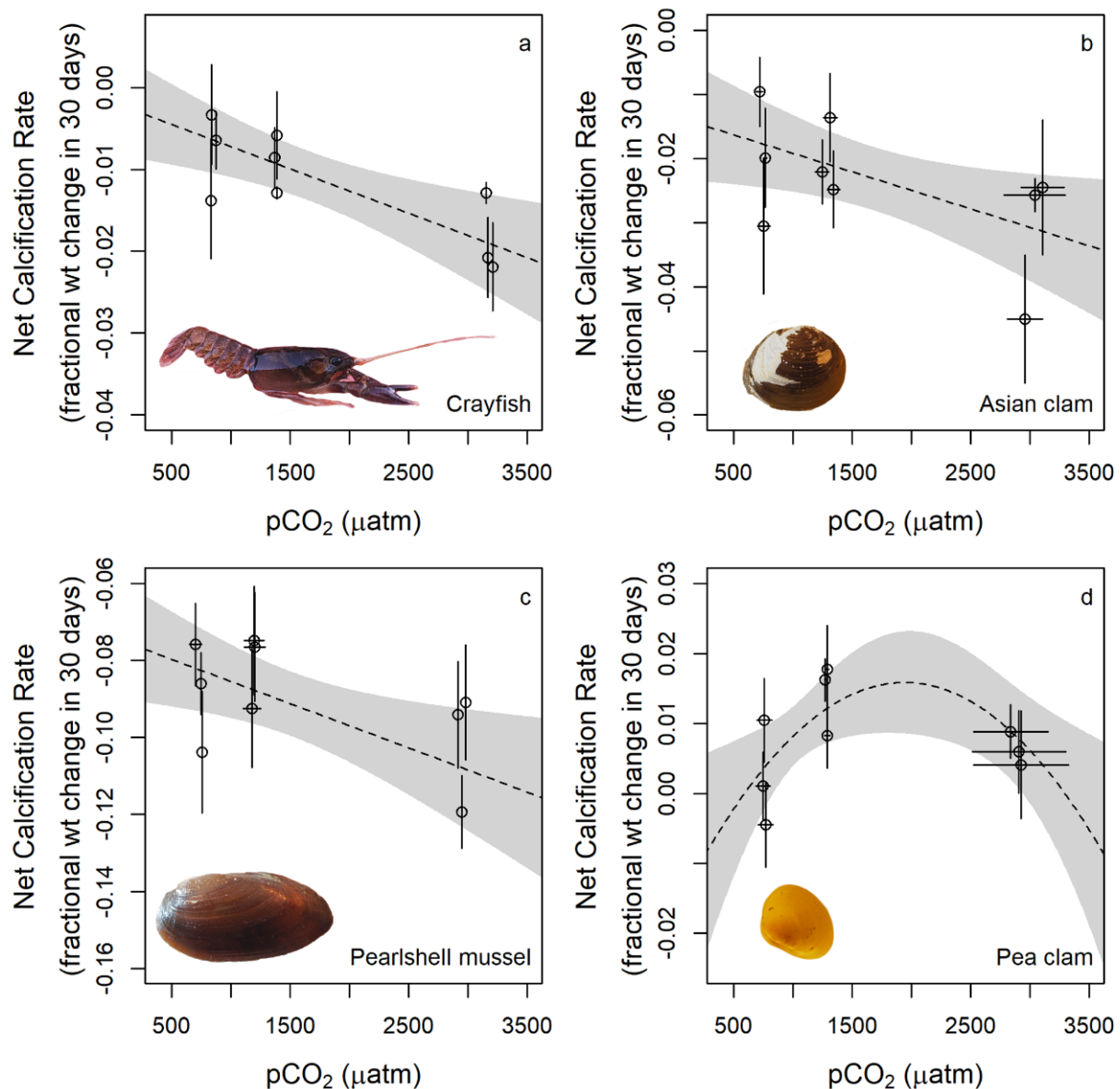
Figure 4. Net calcification rates (expressed as fractional change in buoyant or wet weight normalized

to 30-day growth interval) as a function of water pH for (**a**) the signal crayfish, *Pacifastacus leniusculus* (n = 33, 2−6 individuals per tank); (**b**) the Asian clam, *Corbicula fluminea* (n = 95, 6−15 individuals per tank); (**c**) the Eastern pearlshell mussel, *Margaritifera margaritifera* (n = 62, 2−10 individuals per tank); and (**d**) the pea clam, *Pisidium* sp. (n = 85, 6−15 individuals per tank). All species shown exhibit a linear negative response in net calcification rate to increasing pCO$_2$, except for the pea clam that exhibits a parabolic response. Data markers represent the average net calcification rates for all individuals in each of the three replicate tanks for each of the three pCO$_2$ treatments. Vertical bars represent the standard error of the net calcification rates, while the horizontal bars represent the standard deviation of pCO$_2$ during the incubations. Shaded regions represent the 95% confidence intervals of the best fitting model.

Metabolism and food consumption of the crayfish, *Pacifasticus leniusculus*, exhibited more complex responses to altered pCO$_2$ treatments. Respiration rates averaged 14.7 μmol g^{-1} h^{-1} (n = 43 crayfish, 13 in low and high pCO$_2$ treatments, respectively, 17 in the intermediate pCO$_2$ treatment), but did not vary with pCO$_2$ (Figure 5a, $F_{1,41}$ = 0.281, p = 0.60). Feeding rates, however, were impacted by pCO$_2$ (Figure 5b, ANOVA, $F_{2,15}$ = 4.47, p = 0.030), such that feeding rates in the highest pCO$_2$ trials were significantly less than in the intermediate pCO$_2$ trials (post-hoc Tukey, p = 0.043), and with nearly significantly less than in the lowest pCO$_2$ trials (post-hoc Tukey, p = 0.060).
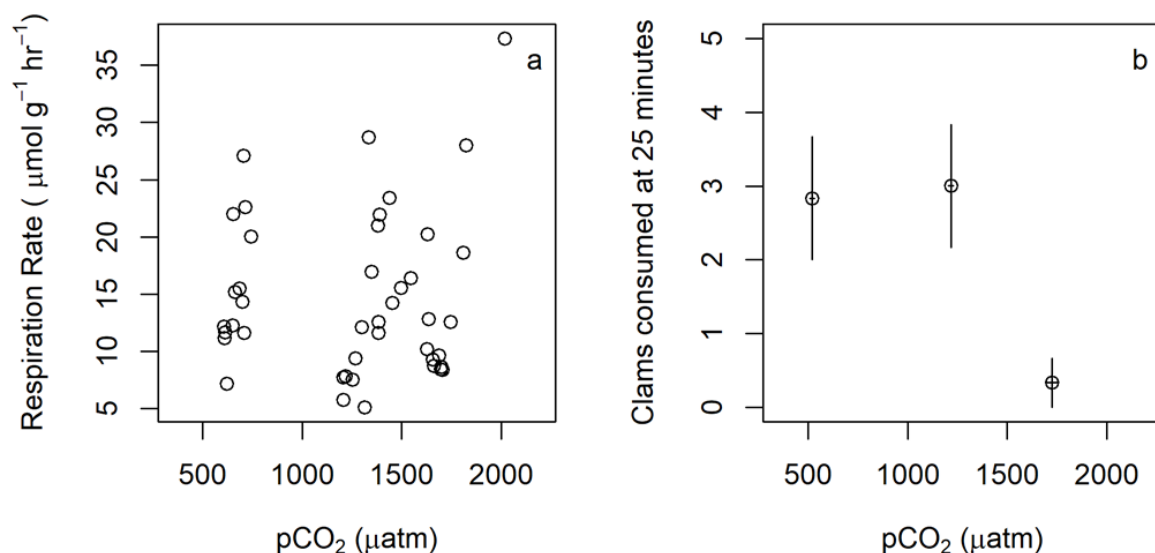
Figure 5. (**a**) Respiration and (**b**) feeding rates of the signal crayfish as a function of pCO$_2$. High pCO$_2$ inhibits feedings rates for the crayfish, while respiration rates do not significantly vary across pCO$_2$ treatments. Vertical bars represent standard error of respiration rates for of feeding rates for six crayfish per treatment; horizontal bars represent standard deviation of pCO$_2$ for the respective treatments.

4. Discussion

Elevated pCO$_2$, resulting in decreased pH, caused a reduction in net calcification rates in three species of freshwater calicifiers, the Asian clam *Corbicula fluminea*, the pearlshell mussel *Margaritifera margaritifera*, and the crayfish *Pacifastacus leniusculus*. In the pea clam, *Pisidium* sp., however, net calcification rate was highest under intermediate pCO$_2$. The linearly negative response of the Asian clam, pearlshell mussel, and crayfish suggests that these species will be negatively impacted by CO$_2$-induced acidification of freshwater systems over the coming decades. However, optimization of calcification under moderate acidification exhibited by the pea clam suggests that this species may be more resilient to CO$_2$-induced acidification predicted for the near future, but this resilience may diminish at higher pCO$_2$ conditions predicted for the next century or two. Although the high inter-specimen variability in growth rates of the pea clam may argue for selection of a simpler

model (i.e., linear), the large number of individuals employed in the pea clam experiment (85) supports adoption of the more complex parabolic model.

There are various mechanisms that can lead to the observed functional relationships between net calcification rate and pCO_2. Because we did not manipulate calcium ion concentrations, shell formation here is likely the culmination of two main processes the uptake of inorganic carbon, primarily in the form of bicarbonate ion and, to a lesser extent, aqueous CO_2, and the efflux of protons (H^+) from the site of calcification that effectively converts bicarbonate ion to carbonate ion available for calcification [18,19]. The linear reduction in net calcification rate with decreased pH (increased pCO_2) exhibited by the Asian clam, pearlshell mussel, and crayfish suggests that these species are limited in their ability to control carbonate chemistry at the site of calcification in support of calcification, such as by removing H^+ from their calcifying fluid.

This linear negative calcification response to elevated pCO_2 exhibited by the crayfish is somewhat surprising given that various species of marine decapod crustacea are reported to calcify faster under elevated pCO_2 [5,20], suggesting that freshwater crustacea utilize dissolved inorganic carbon in shell formation differently than marine crustacea and/or that other processes within their physiological repertoire are more sensitive to pH (see discussion below). The parabolic relationship between net calcification rate and pH exhibited by the pea clam suggests that it may be able to utilize the additional dissolved inorganic carbon (DIC) resulting from increased pCO_2 by, for example, converting it to carbonate ions by removing protons from the site of calcification. Under the highest pCO_2 condition, it is possible that the benefits of this process are overwhelmed by other processes that are more deleteriously impacted by the low pH conditions, such as the dissolution of pre-formed, exposed shell in water that is relatively undersaturated with respect to the clam's aragonite [21] shell mineral. This trend may be further reinforced by nonlinearities imposed by scaling differences between surface- vs. volume-related processes. For example, because *Pisidium* sp. broods its larvae [22], calcification occurs throughout the clam's body cavity as its offspring build their shells. This contrasts the calcification processes of *M. margaritifera* and *C. fluminea*, which do not brood their calcifying offspring. Dissolution, however, acts only on shell surfaces exposed to water with a low saturation state, meaning that the brooding larval *Pisidium* sp. are potentially shielded from this process, which may confer some resilience to calcification of the whole pea clam (i.e., both adults and brooded larvae) under intermediate pCO_2 conditions, potentially resulting in their observed parabolic responses to elevated pCO_2.

It is also possible that decreased water pH impacts rates of shell formation indirectly, potentially through physiological processes beyond biocalcification. For the crayfish, *P. leniusculus*, we observed that feeding rates were reduced at the lowest pH despite no pH-dependent variation in respiration rates. We did not test for specific mechanisms, but similar reductions in feeding rates, arising from modified behavior, have been observed for marine decapods exposed to increased pCO_2 [23]. Alternatively, lowered pH has been shown to cause a biomechanical weakening of the exoskeleton in some species of marine crustacea [24], and it is possible that this could impair their ability to handle and consume prey. Regardless of the cause, these reduced feeding rates under CO_2-induced reductions in water pH would yield less food and energy for shell production by the crayfish, potentially contributing to or driving their linear decline in net calcification rate with increasing pCO_2. Although the feeding rates of the other species were not quantified in the present study, obtaining these types of measurements in future experiments should provide valuable insight into the mechanisms responsible for the observed reductions in net calcification rate of freshwater calcifiers under conditions of elevated pCO_2.

Anthropogenic increases in atmospheric pCO_2 and the resulting decrease in freshwater pH has the potential to negatively impact freshwater aquatic ecosystems by altering the net calcification rate and behavior of calcifying invertebrates [1]. Differential sensitivities to CO_2-induced changes in water chemistry can further shape populations, communities, and ecosystems [25]. Given the ecological importance of freshwater calcifiers in lakes,

ponds, rivers, and streams [26–28], further research is merited to determine the range of responses that such species exhibit to elevated atmospheric pCO_2, and the mechanisms driving these diverse responses. A better understanding of how freshwater species perform under acidification can help inform strategies for managing freshwater systems amidst the various threats that they face, including species invasion, eutrophication, sedimentation, warming, and CO_2-induced acidification.

5. Conclusions

1. CO_2-induced acidification (doubling, quadrupling of ambient pCO_2 causing pH decline of between 0.23 and 0.57 units) caused negative linear calcification responses in three species of freshwater calcifiers and a more complex parabolic calcification response in one species (pea clam). Increased pCO_2 decreased the feeding rates of the signal crayfish on its natural pea clam prey but had no significant impact on crayfish respiration rate (i.e., constant metabolism), potentially driving this species' negative calcification response to acidification by depriving it of energy required for its molt-mediated calcification.
2. Although increased pCO_2 can impair calcification rates of freshwater organisms, variation in these effects amongst species, combined with impacts on predator–prey dynamics, could yield complex ecological consequences for freshwater systems.
3. Results highlight the importance of further elucidating the understudied effects of CO_2-induced acidification within freshwater systems.

Author Contributions: Conceptualization, A.T.N. and J.R.; data curation, A.T.N. and J.R.; formal analysis, A.T.N. and J.R.; funding acquisition, A.T.N. and J.R.; investigation, A.T.N. and J.R.; methodology, A.T.N. and J.R.; resources, A.T.N. and J.R.; writing—original draft, A.T.N. and J.R.; writing—review and editing, A.T.N. and J.R. All authors have read and agreed to the published version of the manuscript.

Funding: A.T.N. was supported by a Russel J. and Dorothy S. Bilinski Fellowship at Bodega Marine Laboratory. J.R. and this research were supported by MIT Sea Grant award no. NA18OAR4170105, by Northeastern's Interdisciplinary Sabbatical Program, by J.R.'s overhead return fund at Northeastern, and by J.R.'s personal funds. J.R. was also supported by the University of California at Davis Tahoe Environmental Research Center, which provided space, equipment, analytical resources, utilities, and boat/dive time in support of this research.

Institutional Review Board Statement: Not applicable.

Informed Consent Statement: Not applicable.

Data Availability Statement: Data available upon request from the authors.

Acknowledgments: We are grateful to numerous scientists and staff members at the UC Davis Tahoe Environmental Research Center (TERC), including Anne Liston, Brant Allen, Katie Senft, and Brandon Berry, for their assistance in the laboratory and with collections in the field, and to TERC Director Geoffrey Schladow for hosting J.R.'s sabbatical and A.T.N.'s visiting appointment and for generously providing resources in support of this work. We are also grateful to Brian Gaylord for advice and comments on previous versions of the manuscript and to Cary and Cindy Ninokawa for their assistance with crayfish collection and feeding trials.

Conflicts of Interest: The authors are not aware of any conflict of interest. Additionally, the external funders had no role in the design of the study; in the collection, analyses, or interpretation of data; in the writing of the manuscript; or in the decision to publish the results.

References

1. Doney, S.C.; Busch, D.S.; Cooley, S.R.; Kroeker, K.J. The impacts of ocean acidification on marine ecosystems and reliant human communities. *Annu. Rev. Environ. Resour.* **2020**, *45*, 1–30. [CrossRef]
2. Hurd, C.L.; Beardall, J.; Comeau, S.; Cornwall, C.E.; Havenhand, J.N.; Munday, P.L.; Parker, L.M.; Raven, J.A.; McGraw, C.M. Ocean acidification as a multiple driver: How interactions between changing seawater carbonate parameters affect marine life. *Mar. Freshw. Res.* **2020**, *71*, 263–274. [CrossRef]

3.   Comeau, S.; Cornwall, C.E.; DeCarlo, T.M.; Krieger, E.; McCulloch, M.T. Similar controls on calcification under ocean acidification across unrelated coral reef taxa. *Glob. Chang. Biol.* **2018**, *24*, 4857–4868. [CrossRef]

4.   Gilbert, P.U.P.A.; Bergmann, K.D.; Boekelheide, N.; Tambutté, S.; Mass, T.; Marin, F.; Adkins, J.F.; Erez, J.; Gilbert, B.; Knutson, V.; et al. Biomineralization: Integrating mechanism and evolutionary history. *Sci. Adv.* **2022**, *8*, eabl9653. [CrossRef]

5.   Ries, J.B.; Cohen, A.L.; McCorkle, D.C. Marine calcifiers exhibit mixed responses to CO_2-induced ocean acidification. *Geology* **2009**, *37*, 1131–1134. [CrossRef]

6.   Gaylord, B.; Barclay, K.M.; Jellison, B.M.; Jurgens, L.J.; Ninokawa, A.T.; Rivest, E.B.; Leighton, L.R. Ocean change within shoreline communities: From biomechanics to behaviour and beyond. *Conserv. Physiol.* **2019**, *7*, 1–14. [CrossRef]

7.   George, M.N.; O'Donnell, M.J.; Concodello, M.; Carrington, E. Mussels repair shell damage despite limitations imposed by ocean acidification. *J. Mar. Sci. Eng.* **2022**, *10*, 359. [CrossRef]

8.   Waldbusser, G.G.; Gray, M.W.; Hales, B.; Langdon, C.J.; Haley, B.A.; Gimenez, I.; Smith, S.R.; Brunner, E.L.; Hutchinson, G. Slow shell building, a possible trait for resistance to the effects of acute ocean acidification. *Limnol. Oceanogr.* **2016**, *61*, 1969–1983. [CrossRef]

9.   Jokiel, P.L. Ocean acidification and control of reef coral calcification by boundary layer limitation of proton flux. *Bull. Mar. Sci.* **2011**, *87*, 639–657. [CrossRef]

10.   Hasler, C.T.; Butman, D.; Jeffrey, J.D.; Suski, C.D. Freshwater biota and rising pCO_2? *Ecol. Lett.* **2016**, *19*, 98–108. [CrossRef] [PubMed]

11.   Aufdenkampe, A.K.; Mayorga, E.; Raymond, P.A.; Melack, J.M.; Doney, S.C.; Alin, S.R.; Aalto, R.E.; Yoo, K. Riverine coupling of biogeochemical cycles between land, oceans, and atmosphere. *Front. Ecol. Environ.* **2011**, *9*, 53–60. [CrossRef]

12.   Hasler, C.T.; Jeffrey, J.D.; Schneider, E.V.C.; Hannan, K.D.; Tix, J.A.; Suski, C.D. Biological consequences of weak acidification caused by elevated carbon dioxide in freshwater ecosystems. *Hydrobiologia* **2018**, *806*, 1–12. [CrossRef]

13.   Caldeira, K.; Wickett, M. Ocean model predictions of chemistry changes from carbon dioxide emissions to the atmosphere and ocean. *J. Geophys. Res. C Ocean.* **2005**, *110*, 1–12. [CrossRef]

14.   Waters, J.; Millero, F.J.; Woosley, R.J. Corrigendum to "The free proton concentration scale for seawater pH", [MARCHE: 149 (2013) 8-22]. *Mar. Chem.* **2014**, *165*, 66–67. [CrossRef]

15.   Nathenson, M. *Chemistry of Lake Tahoe, California-Nevada, and Nearby Springs*; Department of the Interior, US Geological Survey: Reston, VA, USA, 1989. [CrossRef]

16.   Jokiel, P. Coral growth: Buoyant weight. In *Coral Reefs: Research Methods*; Stoddart, D.R., Johannes, R.E., Eds.; UNESCO: Paris, France, 1978; pp. 529–541.

17.   Shechter, A.; Berman, A.; Singer, A.; Freiman, A.; Grinstein, M.; Erez, J.; Aflalo, E.D.; Sagi, A. Reciprocal changes in calcification of the gastrolith and cuticle during the molt cycle of the red claw crayfish *Cherax quadricarinatus*. *Biol. Bull.* **2008**, *214*, 122–134. [CrossRef] [PubMed]

18.   Bach, L.T. Reconsidering the role of carbonate ion concentration in calcification by marine organisms. *Biogeosciences* **2015**, *12*, 4939–4951. [CrossRef]

19.   Liu, Y.W.; Sutton, J.N.; Ries, J.B.; Eagle, R.A. Regulation of calcification site pH is a polyphyletic but not always governing response to ocean acidification. *Sci. Adv.* **2020**, *6*, eaax1314. [CrossRef]

20.   Kroeker, K.J.; Kordas, R.L.; Crim, R.N.; Singh, G.G. Meta-analysis reveals negative yet variable effects of ocean acidification on marine organisms. *Ecol. Lett.* **2010**, *13*, 1419–1434. [CrossRef]

21.   Cummings, K.S.; Graf, D.L. Mollusca: Bivalvia. In *Ecology and Classification of North American Freshwater Invertebrates*; Thorp, J.H., Covich, A.P., Eds.; Elsevier: London, UK, 2010; pp. 309–384. ISBN 978-0-12-374855-3.

22.   Guralnick, R. Life-history patterns in the brooding freshwater bivalve Pisidium (*Sphaeriidae*). *J. Molluscan Stud.* **2004**, *70*, 341–351. [CrossRef]

23.   Dodd, L.F.; Grabowski, J.H.; Piehler, M.F.; Westfield, I.; Ries, J.B. Ocean acidification impairs crab foraging behavior. *Proc. R. Soc. B Biol. Sci.* **2015**, *282*, 1–9. [CrossRef]

24.   Dickinson, G.H.; Bejerano, S.; Salvador, T.; Makdisi, C.; Patel, S.; Long, W.C.; Swiney, K.M.; Foy, R.J.; Steffel, B.V.; Smith, K.E.; et al. Ocean acidification alters properties of the exoskeleton in adult Tanner crabs, *Chionoecetes bairdi*. *J. Exp. Biol.* **2021**, *224*, jeb232819. [CrossRef] [PubMed]

25.   Kroeker, K.J.; Micheli, F.; Gambi, M.C. Ocean acidification causes ecosystem shifts via altered competitive interactions. *Nat. Clim. Chang.* **2013**, *3*, 156–159. [CrossRef]

26.   Dodds, W.K.; Perkin, J.S.; Gerken, J.E. Human impact on freshwater ecosystem services: A global perspective. *Environ. Sci. Technol.* **2013**, *47*, 9061–9068. [CrossRef] [PubMed]

27.   Vaughn, C.C.; Hakenkamp, C.C. The functional role of burrowing bivalves in freshwater ecosystems. *Freshw. Biol.* **2001**, *46*, 1431–1446. [CrossRef]

28.   Reynolds, J.; Souty-Grosset, C.; Richardson, A. Ecological roles of crayfish in freshwater and terrestrial habitats. *Freshw. Crayfish* **2013**, *19*, 197–218. [CrossRef]